Available online at www.sciencedirect.com
ScienceDirect
Journal of Power Sources 159 (2006) 163–166
JOURNAL OF POWER SOURCES
www.elsevier.com/locate/jpowsour

Short communication

Hydrogen storage properties of nanocrystalline Mg–Ce/Ni composite

X.L. Wang [a], J.P. Tu [a,*], C.H. Wang [b], X.B. Zhang [a], C.P. Chen [a], X.B. Zhao [a]

[a] *Department of Materials Science and Engineering, Zhejiang University, Hangzhou 310027, China*
[b] *Zhejiang Research Institute of Mechanical and Electrical Engineering Co. Ltd., Hangzhou 310009, China*

Available online 23 May 2006

Abstract

Mg–Ce alloy was prepared by induction melting under vacuum, hydrided firstly and then Mg–Ce/Ni composite was obtained by mechanical milling Mg–Ce hydrides under Ar for 50 h with addition of nano-sized Ni powder. XRD results showed $CeMg_{12}$ formed in melted alloy. $CeMg_{12}$ disappeared and $CeH_{2.53}$ emerged during subsequent hydriding. The phase composition was not changed during ball milling process. Compared with Mg and Mg/Ni, Mg–Ce/Ni composite showed significant hydriding/dehydriding performance without any prior activation. The enthalpy of hydride formation for Mg–10.9 wt.% Ce/10 wt.% Ni composite was $-70.58\,kJ\,mol^{-1}$ H_2. Improved hydrogen storage properties were attributed to the catalytic effect of addition of nano-sized Ni particles and existence of $CeH_{2.53}$, as well as the grain refinement, defects, etc. in the material introduced by ball milling process.

Keywords: Hydrogen storage; Mg-based composite; Ball milling; Reaction kinetics

1. Introduction

Many metal-hydrogen systems have been proposed as hydrogen storage materials. Among them, the Mg-based alloys are considered as potential candidates for hydrogen storage materials for their large hydrogen capacity and low cost [1,2]. However, as Mg-based alloys desorb hydrogen at temperatures higher than 600 K, they are not applicable to practical use. Therefore, how to destabilize their hydrides are the main objectives in this research field.

Improvement of the kinetics and modification of the dissociation temperature or the plateau pressure can be obtained by either chemical alloying (e.g. substitution or addition of other elements) or through material processing (e.g. melt spinning, mechanical alloying) [3–6]. Mechanical alloying as a solid-state processing technique provides significant potential for both alloying and microstructural modifications of hydrogen storage material. The formation of nano-sized particles with clean surfaces also enhances the hydriding/dehydriding kinetics. Hence, mechanically alloying Mg with other transition metals can increase the maximum solubility, produce fine particles in the submicrometer or even nanometer size range, create fresh surfaces and homogeneously dispersed nanometer particles within Mg particles [7].

For increasing the capacity, the RE–Mg–Ni systems alloy is one of the promising candidates. Among these systems, RE elements addition played critical roles for improving the hydrogenation properties [8,9]. In this work, the hydrogen storage properties Mg–10.9 wt.% Ce/10.0 wt.% Ni composite was investigated.

2. Experimental details

Mg–10.9 wt.% Ce alloy was prepared by induction melting under vacuum and then mechanically pulverized. Because of the high ductility of Mg alloy, the as-melted alloy powder was preliminary hydrided at 613 K under the hydrogen pressure of 4.0 MPa in order to make finer powder. Thereafter, Mg hydrides, Mg hydrides with 10.0 wt.% Ni and Mg–10.9 wt.% Ce hydrides with 10.0 wt.% Ni were put into the stainless steel vial with argon as protection atmosphere, respectively. Ball milling process was carried out for 50 h with a ball to powder ration of 50:1 at rotating speed of 280 rpm. It should be noted that Ni powder used here was nano-scaled particles prepared through $Ni(CH_3COO)_2$ being deoxidized by KBH_4. And the average grain size of Ni particles obtained was 10 nm. The composite powders resulted from the milling were characterized by X-ray diffraction (XRD) and scanning electron microscopy (SEM).

* Corresponding author. Tel.: +86 571 87952573; fax: +86 571 87952856.
E-mail address: tujp@zju.edu.cn (J.P. Tu).

0378-7753/$ – see front matter © 2006 Elsevier B.V. All rights reserved.
doi:10.1016/j.jpowsour.2006.04.014

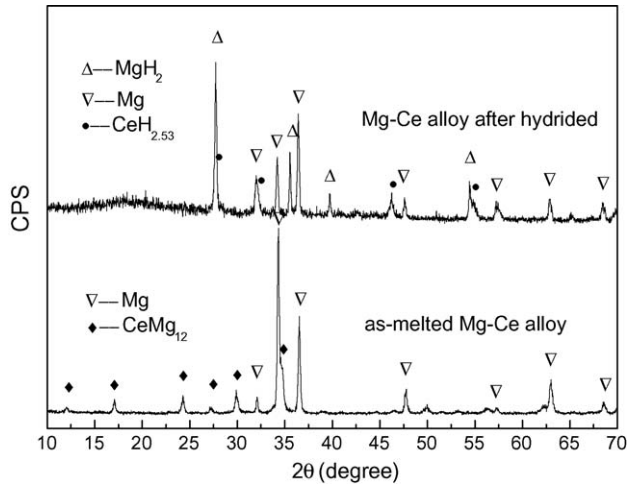

Fig. 1. XRD patterns of Mg–Ce alloy before and after hydrided.

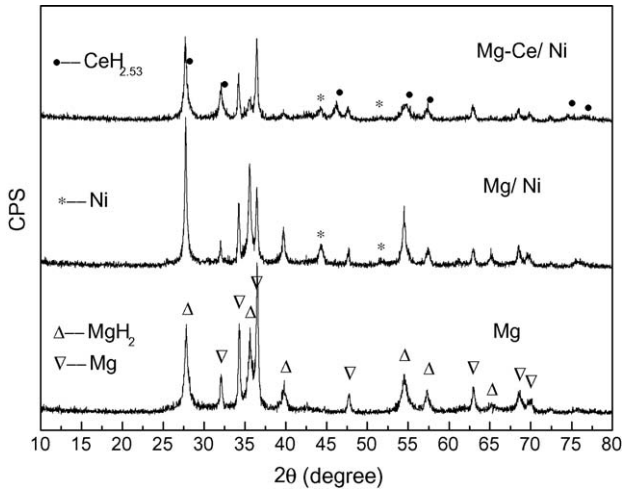

Fig. 2. XRD patterns of Mg, Mg/Ni and Mg–Ce/Ni hydrides after ball milling for 50 h.

Measurement of hydriding/dehydriding kinetics of the as-milled samples was similar to what described in Ref. [10]. Pressure–composition isotherms (*P–C–T* diagrams) of Mg–Ce/Ni powders were also measured at 553, 573 and 613 K, respectively, so that to estimate the enthalpy of hydride formation.

3. Results and discussion

Fig. 1 shows the XRD patterns of as-melted Mg–10.9 wt.% Ce alloy before and after hydrided. For the melted alloy, Ce alloyed with partial Mg and $CeMg_{12}$ ($a = 10.307$ (1), $b = 10.307$ (1), $c = 10.409$ (1), $P6_3/mmc$) phase was formed. The content of $CeMg_{12}$ phase was 44.32 wt.% estimated through structure refinement and profile matching. After reacted with hydrogen at 613 K, $CeMg_{12}$ phase disappeared and $CeH_{2.53}$ phase emerged by the reaction of $2CeMg_{12} + xH_2 \rightarrow 2CeH_x + 24Mg$. Besides, Mg partly reacted with hydrogen and some single Mg still existed, indicating that the melted Mg–Ce alloy could not be hydrided completely even at 613 K. From the XRD patterns of Mg hydrides after ball milling for 50 h, as shown in Fig. 2, it can be seen that the diffraction peaks were broadened because of the particle refinement, defects and the intrinsic stress accumulation during long-time mechanical milling. It should be noted that nano-scaled Ni particles here did not react with Mg or MgH_2 during mechanical milling and still remained pure Ni phase, which is different from what reported [11]. As shown in Fig. 3, the SEM micrographs of the ball-milled composites showed the particle size of Mg–10.9 wt.% Ce/10 wt.% Ni is smallest which is in accordance with Fig. 2. Besides, in the case of the addition of both Ce and Ni, the ball-milled sample showed more like the slice than the reunited blocks.

Fig. 4 presents the hydrogen absorption kinetics of the ball-milled samples at different temperatures. The addition of nano-scaled Ni and Ce here improved the hydriding kinetics greatly, especially at the temperatures below 433 K. Pure Mg hardly reacted with hydrogen at 393 K, while the hydrogen storage capacity of Mg/10 wt.% Ni could reach 2.09 wt.% and Mg–10.9 wt.% Ce/10 wt.% Ni composite could absorb 2.92 wt.% H (Fig. 5) at the same temperature. It should be noted that the addition of Ni and Ce could also improve the activation properties of Mg-based hydrogen storage material. Pure Mg needed three hydriding/dehydriding cycles to reach the maximum hydrogen absorption capacity. However, both Mg/10 wt.% Ni and Mg–10.9 wt.% Ce/10 wt.% Ni could reach the maximum hydrogen absorption capacity without any prior activation. And all the hydriding process could be finished in 3 min. The maximum hydrogen storage capacity increased with increasing temperature (Table 1). For hydrogen desorption side, the dehy-

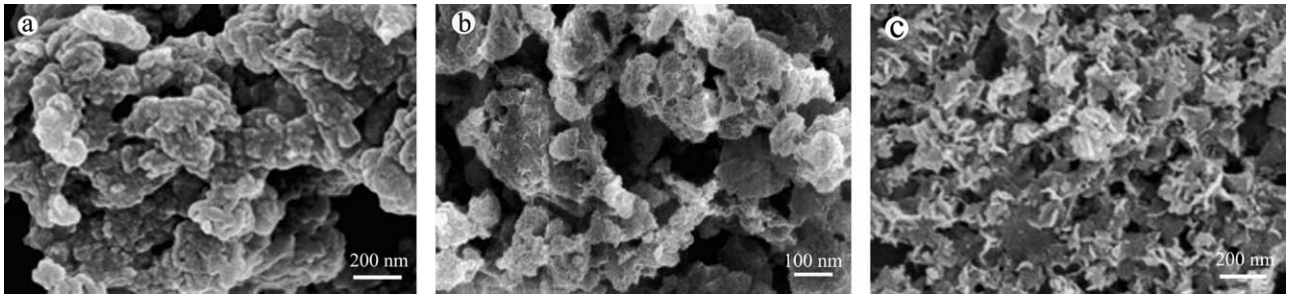

Fig. 3. SEM micrographs of the ball-milled composites. (a) Mg; (b) Mg–10 wt.% Ni; (c) Mg–10.9 wt.% Ce/10 wt.% Ni.

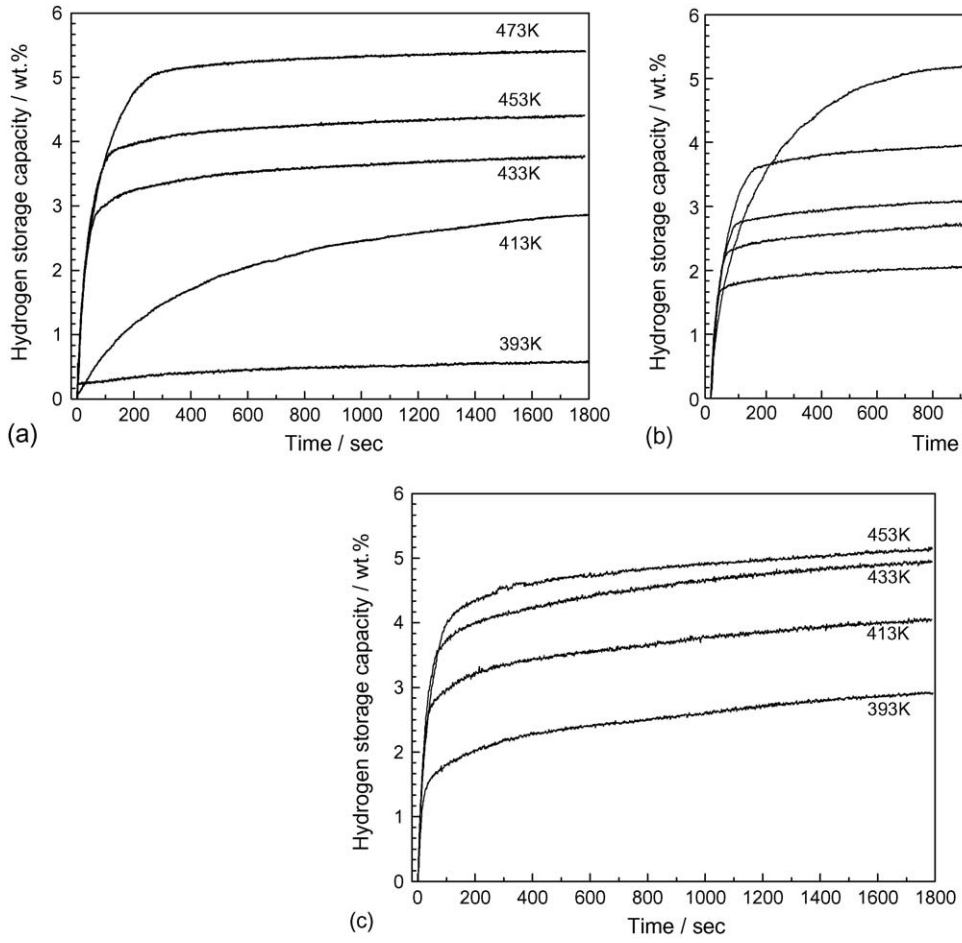

Fig. 4. Absorption kinetics of samples at different temperatures under initial 4 MPa H_2. (a) Mg; (b) Mg/10 wt.% Ni; (c) Mg–10.9 wt.% Ce/10 wt.%Ni.

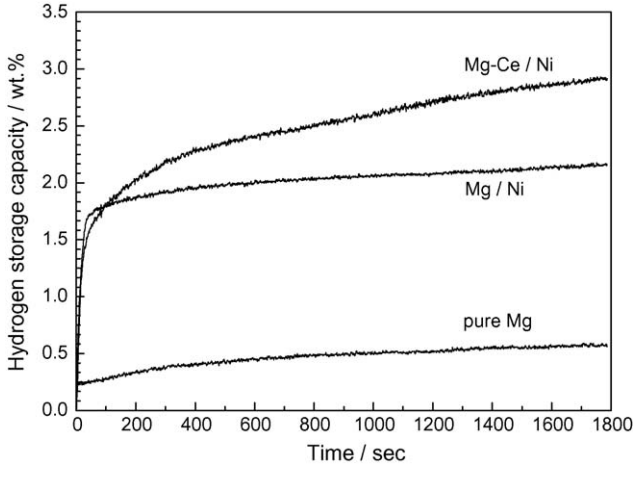

Fig. 5. Absorption kinetics of ball-milled samples at 393 K under initial 4 MPa H_2.

Table 1
Maximum hydrogen storage capacity of samples at different temperatures

Sample	393 K	413 K	433 K	453 K	473 K
Mg	0.57	2.85	3.76	4.40	5.39
Mg/10.0 wt.% Ni	2.16	2.88	3.18	4.12	5.33
Mg–10.9 wt.% Ce/10.0 wt.% Ni	2.92	4.05	4.94	5.30	–

driding temperature was decreased with the addition of both Ce and Ni. As is that pure Mg and Mg/10 wt.% Mi began to desorb hydrogen at 473 K while Mg–10.9 wt.% Ce/10 wt.% Ni could desorb hydrogen at 433 K at slow rate. The hydrogen desorption kinetics at 453 K under H_2 pressure of 0.1 MPa is shown in Fig. 6. Desorbed hydrogen content reached 2.12 wt.%

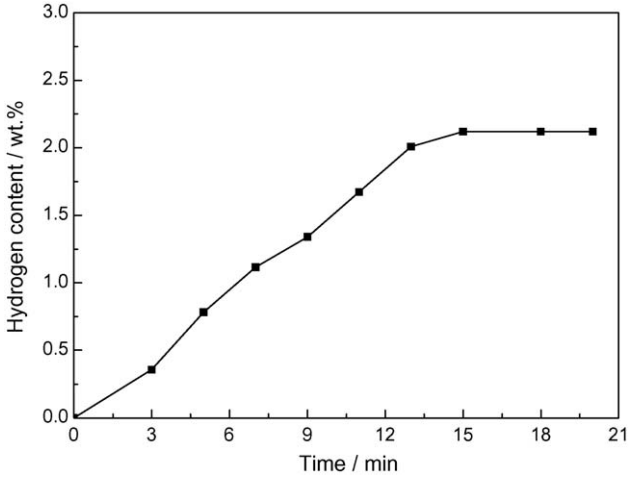

Fig. 6. Desorption kinetics of Mg–Ce/Ni composite at 453 K under 0.1 MPa H_2.

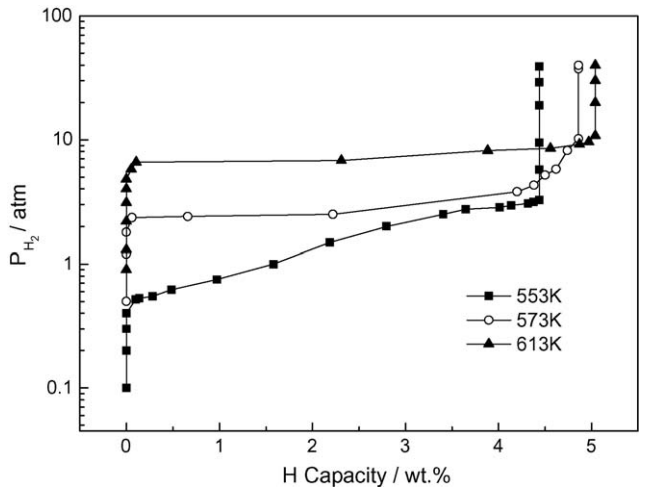

Fig. 7. *P–C–T* absorption curves of Mg–Ce/Ni composite.

within 20 min. To understand the hydrogen storage characteristics of Mg–10.9 wt.% Ce/10 wt.% Ni composite, the absorption pressure–composition isotherms were generated at different temperatures. As shown in Fig. 7, each of the *P–C–T* curves show a single plateau region, indicating that only one phase takes part in hydrogen absorption. The absorption enthalpies of hydrides formation is $-70.58\,kJ\,mol^{-1}$ H_2 measured by Van't Hoff plots. It is smaller than that of pure MgH_2 ($-74\,kJ\,mol^{-1}$ H_2) [12].

The interface between Mg–Mg, Mg–$CeH_{2.53}$ and Mg–Ni acts as an active nucleation site for the MgH_2. Zaluska et al. pointed out that the efficiency of the catalyst depends critically on how well it is dispersed through the system [13]. And for this reason the best efficiency of solid-state catalyst is obtained when catalyst particles are as small as possible. In the present work, the nano-sized Ni acted as catalyst for hydriding can improve the efficiency of Ni catalyst. It is reported [14] that the nickel particles inlaid on the surface of nanocrystalline Mg alloy may also act as the active sites for the redox reaction of hydrogen and at the same time have the "bypass effect" for hydrogen diffusion. Furthermore, mechanical milling can facilitate nucleation by creating many defects on the surface and/or in the interior of Mg, or by an additive acting as active sites for the nucleation, and shortened diffusion distance by reducing the effective particle sizes of Mg. Compared with Mg/10.0 wt.% Ni, the Mg–10.9 wt.% Ce/10.0 wt.% Ni composite showed better hydrogen absorption properties (Table 1). Liang et al. [15] reported that La_2Mg_{17} undergoes disproportion reaction on hydrogenation: $La_2Mg_{17} + 20H_2 \rightarrow LaH_x + Mg$, and La hydride is not reversible. Besides, LaH_{2+c} and CeH_{2+c} are structurally similar [16]. We deduced that $CeH_{2.53}$ in this work did not react with hydrogen reversibly during hydring/dehydring process and it acted as catalyst, which was according to only one plateau in the *P–C–T* diagrams of composite. All those mentioned above resulted in the improved hydrogen storage performance.

4. Conclusion

Mg–Ce alloy was prepared by induction melting under vacuum, hydrided firstly and then Mg–Ce/Ni composite was obtained by ball milling Mg–Ce hydrides under Ar for 50 h with addition of nano-sized Ni powder. XRD results showed $CeMg_{12}$ formed in melted alloy. $CeMg_{12}$ disappeared and $CeH_{2.53}$ emerged during subsequent hydriding at 613 K. Ball milling process did not change the phase composition. Compared with Mg and Mg/Ni, Mg–Ce/Ni composite showed significant hydriding/dehydriding performance without any prior activation. The Mg–Ce/Ni composite could absorb 2.92 wt.% H at 393 K. Besides, it could desorb 2.12 wt.% H at 453 K under 0.1 MPa H_2 pressure. The enthalpy of hydride formation for Mg–Ce/Ni composite was $-70.58\,kJ\,mol^{-1}$ H_2 measured by Van't Hoff plots. The improved hydrogen storage properties were attributed to the catalytic effect of the addition of nano-sized Ni particles and existence of $CeH_{2.53}$, as well as the grain refinement, defects, etc. in the material introduced by ball milling process.

Acknowledgement

This work was supported by the special Funds for Major States Basic Research Project (no. TG20000264-06) of MOST, China.

References

[1] J.J. Reilly, R.H. Wiswall, Inorg. Chem. 7 (1968) 2254–2256.
[2] H.G. Schimmel, M.R. Johnson, G.J. Kearley, A.J. Ramirez-Cuesta, J. Huot, F.M. Mulder, Mater. Sci. Eng. B 108 (2004) 38–41.
[3] J.C. Bolcich, A.A. Yawny, H.L. Corso, H.A. Peretti, C.O. Ayala, Int. J. Hydrogen Energy 19 (7) (1994) 605–609.
[4] Y. Nakamori, G. Kitahara, S. Orimo, J. Power Sources 138 (2004) 309–312.
[5] H. Imamura, K. Masanari, M. Kusuhara, H. Katsumoto, T. Sumi, Y. Sakata, J. Alloys Compd. 386 (2005) 211–216.
[6] C.X. Shang, Z.X. Guo, J. Power Sources 129 (2004) 73–80.
[7] L.E.A. Berlouis, R. Perez Aguado, P.J. Hall, S. Morris, L. Chandrasekaran, S.B. Dodd, J. Alloys Compd. 356/357 (2003) 584–587.
[8] W. Wang, C.P. Chen, L.X. Chen, Q.D. Wang, J. Alloys Compd. 339 (2002) 175–179.
[9] D. Sun, F. Gingl, H. Enoki, D.K. Ross, E. Akiba, Acta Mater. 48 (2000) 2363–2372.
[10] R.G. Gao, J.P. Tu, X.L. Wang, X.B. Zhang, C.P. Chen, J. Alloys Compd. 356/357 (2003) 649–653.
[11] G. Liang, J. Huot, S. Boily, A. Van Neste, R. Schlz, J. Alloys Compd. 297 (2000) 261–265.
[12] J.F. Stampfer Jr., C.E. Holley Jr., J.F. Suttle, J. Am. Chem. Soc. 82 (1960) 3504–3508.
[13] A. Zaluska, L. Zaluski, J.O. StrÖm-Olsen, Appl. Phys. A 72 (2001) 157–165.
[14] N. Cui, P. He, J.L. Luo, Electrochim. Acta 44 (1999) 3549–3558.
[15] G. Liang, S. Boily, J. Huot, A. Van Neste, R. Schulz, J. Alloys Compd. 268 (1998) 302–307.
[16] I. Ratishvili, N. Namoradze, J. Alloys Compd. 356/357 (2003) 87–90.